SIX-CABLE ROBOCRANE ADAPTED TO EIGHT CABLES

Robert L. Williams II*[1] and Eric Graf[1]

[1]*Department of Mechanical Engineering, Ohio University, Athens, Ohio, USA.

ABSTRACT
This paper presents extension of the triangular 6-cable NIST RoboCrane to a rectangular 8-cable-suspended robot, motivated by an application in the ARGOS (Active Response Gravity Offload System) Laboratory at NASA Johnson Space Center. Six candidate cable/platform design arrangements are considered and evaluated in MATLAB simulation, based on all-eight-cable-positive tensions workspace, singularities, magnitude and slope of cable tensions during trajectories, translational/rotational stiffness, and cable interference. As ever in engineering design, there are tradeoffs, and recommendations are made as to the most suitable design out of the six candidates.

KEYWORDS
Cable-suspended robot, NIST RoboCrane, Eight cables, Pseudostatics, Positive cable tensions, Singularities, Stiffness and Cable interference.

Author for Correspondence:

Robert L. Williams II,

Department of Mechanical Engineering,

Ohio University,

Athens OH 45701, USA.

Email: williar4@ohio.edu

INTRODUCTION
The Active Response Gravity Offload System (ARGOS, Figure No.1) is used at NASA's Johnson Space Center for experimental simulations of reduced gravity on humans and vehicles for planetary exploration. This paper analyzes the potential use of a cable-suspended robot system in place of the current single cable system, providing the system with additional capabilities for gravity simulation not possible with its current design. The potential of using this cable-suspended robot system is evaluated by kinematic and pseudo static MATLAB simulation. This project is to serve as the ground work for future work in testing and evaluating a cable-suspended robot system as a

replacement to the current ARGOS system. The current cable is 1-dof-controlled and so it can swing freely, being quite under constrained. The NASA JSC ARGOS Laboratory invited us to collaborate on a project updating ARGOS with the triangular 6-cable NIST RoboCrane[1]; we then suggested a rectangular, 8-cable extension of the RoboCrane since this would fit in the ARGOS rectangular workspace much more naturally.

Cable robots have been used for a variety of applications, including material handling, e.g[1-3], haptics[4,5], International Space Station[6], demining[7], and large outdoor construction[8].

Based on the degree to which the cables determine the pose (position and orientation) of the manipulator, cable robots can be put into one of two categories: fully-constrained and under constrained. In the fully-constrained case the pose of the end-effect or can be completely determined given the current lengths of the cables. An example of a fully-constrained cable robot is the FALCON-7[2]. Fully constrained cable robots have been designed for applications that require high precision, high speed/acceleration or high stiffness. Under constrained cable robots have been proposed for contour crafting construction[9]. However, because of the need for large workspace manipulation that has both precise motion and high stiffness, a fully-constrained cable robot is preferable (such as the robot system in this document, i.e. 8 active cables to control 6-dof spatial pose).

The robot previously mentioned for International Space Station application[6], has been used more recently at NASA Johnson Space Center, as a large-satellite-simulating haptic device for VR-based astronaut training. Charlotte has 8 cables, 4 attached to the ceiling and 4 to the floor; cable crossing is employed for better moment feedback. The proposed 8-cable robot in this document is more like an 8-cable rectangular extension of the 6-cable triangular NIST RoboCrane[1], with all 8 cables attaching to the ceiling.

The ARGOS Laboratory occupies a relatively large space (a footprint of 12.5 m x 7.3 m and a height of 7.6 m), but it is indoors, and so ideal, massless, tensioned, straight-line cable models were used

throughout, rather than the complicated cable sag models available wherein the kinematics and statics problems are coupled[10]. The main benefit of our 8-cable RoboCrane extension is that is naturally fits a rectangular room better than the original. The cost is extra motors, cables, and sensors.

This paper presents the 8-cable RoboCrane extension concept, followed by methods, results and discussion, then conclusions, including future work plans.

EIGHT-CABLE-SUSPENDED ROBOT CONCEPT

This paper presents an eight-cable cable-suspended robot concept (Figure No.2a and 2b). It is essentially an 8-cable rectangular extension of the 6-cable triangular RoboCrane. Six design candidates are considered, shown in Figure No.3.

This section describes the Eight-Cable-Suspended Robot concept. Figure No.2b shows the robot kinematic diagram, from the top view. The base Cartesian reference frame is {0}, attached at the ground surface, in the center of the base rectangle, with fixed $\hat{X}_0, \hat{Y}_0, \hat{Z}_0$ coordinate axis directions. The control point is the origin of frame {P}, in the center of the moving platform, as shown. Frame {P} has moving coordinate axis directions $\hat{X}_P, \hat{Y}_P, \hat{Z}_P$. The pose (position and orientation) of {P} is controlled with respect to {0} by coordinating the eight cables.

Each of the eight active cables runs from a fixed overhead-cable-pulley point $B_i, i = 1, 2, 3, 4$, to a moving platform-fixed vertex P_j, $j = 1, 2, 3, 4$, as shown. Each of the eight tensioning torque motors/cable reels is fixed to the base at overhead points B_i. Alternatively, the motors and cable reels could be mounted to the floor, with each drive cable passing over pulleys at B_i. As another alternative, the motors and cable reels could be mounted to the moving platform at vertex points P_j (as in the RoboCrane design[1]). This alternative would increase portability but add significant moving dynamic inertia. The eight cable lengths are L_i, $i = 1, 2, \cdots, 8$. The position vector $\{^0\mathbf{P}_P\} = \{x \quad y \quad z\}^T$ gives the position of control point P with respect to the {0}

origin, expressed in {0} coordinates. The 3D orientations of the platform with respect to the base are expressed by *Z-Y-X* Euler Angles α, β, γ[11]. The platform orientation shown in Figure No.2a and 2b is for all three Euler angles equal to zero. As is standard, here Euler angles indicate rotations about the moving axes.

Design Candidate 1: in-line platform, non-crossed cables (Orientation 1 - Uncrossed Cables)

Design Candidate 2: in-line platform, crossed cables (Orientation 1 - Crossed Cables)

Design Candidate 3: rotated platform, non-crossed cables (Orientation 2 - Uncrossed Cables)

Design Candidate 4: rotated platform, crossed cables (Orientation 2 - Crossed Cables)

Design Candidate 5: square platform, non-crossed cables (Square End-Effector - Uncrossed Cables)

Design Candidate 6: square platform, crossed cables (Square End Effector - Crossed Cables)

This cable-robot system has actuation redundancy since there are eight active cables for six Cartesian motion components. The actuation redundancy will be used to ensure all cables maintain tension at all times, since cables can only exert tension on the moving platform. The gravity loading on the moving platform due to the platform mass will also help to maintain cable tensions for all motions. Despite the actuation redundancy and gravity loading, positions are still possible where one or more cable tensions can go slack, which must be avoided in practical applications. For instance, the moving platform vertices cannot move outside the footprint of the base rectangle. Rotations are even more limited. Positive cable tensions must be ensured for all motion control.

The fixed overhead-cable-pulley points B_i are constant in the base frame {0} and the moving platform vertices P_j are constant in the platform frame {*P*}. The ARGOS workspace has rectangular dimensions *L* x *W* x *H*, and the moving platform has rectangular dimensions *l* x *w* x*h*.

We consider six candidate designs cases for the eight-cable-suspended robot, with in-line vs. rotated platform, and uncrossed vs. crossed cables, and rectangular vs. square end-effector platform. Figure No.3 shows the six design candidates. For now we only consider an end-effector platform with the same

aspect ratio as the base rectangle (1/8 of the base rectangular size), or a square platform with identical area to the rectangular platform.

METHODS
The MATLAB simulations developed to compare the six 8-cable robot design candidates for the purpose of choosing the best one require: 1. Inverse pose kinematics (IPK); 2. Pseudostatics; 3. Stiffness calculations and 4. Cable interference detection.

IPK
The inverse pose kinematics (IPK) problem is stated: Given the desired end-effector pose $\{^0\mathbf{P}_P\} = \{x \quad y \quad z\}^T$ and Euler Angles α, β, γ, calculate the required eight active cable lengths L_i, $i = 1, 2, \cdots, 8$. This IPK solution is required for the simulated trajectories presented later. Like most cable-suspended robots and other parallel robots, the inverse pose kinematics solution is straight-forward since the cable lengths are simply the Euclidean norms of the cable vectors connecting each upper support point with the known platform cable connection points. The cable vertices for the base are known and fixed, while the moving cable vertices for the platform are easily calculated from the given Cartesian pose and the known platform vertices locations in the moving frame. One must express all vectors in the same frame, e.g. {0} for success.

Pseudostatics
In pseudostatics analysis we assume that all moving platform velocities and accelerations (translational and rotational) are sufficiently small to ignore dynamic inertial effects and use the conditions of static equilibrium for all motion snapshots. This analysis is necessary to calculate the cable tensions in each of the eight cables for all motion for all designs considered. Given the platform mass and any external forces/ moments (the external forces/ moments are assumed to be zero in later results), the cable tensions can be calculated and compared with maximum allowable tensions in design. More crucially, this analysis is also required in attempt to maintain only positive cable tensions for all motion, for each design.

The pseudostatics equations and Jacobian matrix are presented below. This was derived from the moving

platform free-body diagram and enforcing conditions of translational and rotational static equilibrium at any general pose.

$$^0[\mathbf{S}]\{\mathbf{t}\} = -\,^0\{\mathbf{W}_{EXT} + \mathbf{G}\} \tag{1}$$

$$^0[\mathbf{S}] = \begin{bmatrix} \hat{\mathbf{L}}_1 & \hat{\mathbf{L}}_2 & \hat{\mathbf{L}}_3 & \hat{\mathbf{L}}_4 & \hat{\mathbf{L}}_5 & \hat{\mathbf{L}}_6 & \hat{\mathbf{L}}_7 & \hat{\mathbf{L}}_8 \\ \mathbf{P}_1 \times \hat{\mathbf{L}}_1 & \mathbf{P}_2 \times \hat{\mathbf{L}}_2 & \mathbf{P}_2 \times \hat{\mathbf{L}}_3 & \mathbf{P}_3 \times \hat{\mathbf{L}}_4 & \mathbf{P}_3 \times \hat{\mathbf{L}}_5 & \mathbf{P}_4 \times \hat{\mathbf{L}}_6 & \mathbf{P}_4 \times \hat{\mathbf{L}}_7 & \mathbf{P}_1 \times \hat{\mathbf{L}}_8 \end{bmatrix} \tag{2}$$

where $^0[\mathbf{S}]$ is the statics Jacobian matrix in $\{0\}$, $\mathbf{P}_j = \{^0\mathbf{P}_j\} = [^0_P\mathbf{R}]\{^P\mathbf{P}_j\}$, $j = 1,2,3,4$, $[^0_P\mathbf{R}]$ is the orthonormal rotation matrix giving the orientation of $\{P\}$ with respect to $\{0\}$ [11], $\hat{\mathbf{L}}_i$ is the unit vector along the ith cable, directed from the platform towards the base, $\{\mathbf{t}\} = \{t_1 \quad t_2 \quad \cdots \quad t_8\}^T$ is the vector of eight cable tensions, $\{\mathbf{W}_{EXT}\} = \{\mathbf{F}_{EXT} \quad \mathbf{M}_{EXT} + \mathbf{r}_{EXT}\mathbf{F}_{EXT}\}^T$ is the external wrench vector, $\mathbf{r}_{EXT}$ is the moment arm vector from the moment center to the point of application of the external force, and $\{\mathbf{G}\} = \{m\mathbf{g} \quad ^0_P\mathbf{R}\,^P\mathbf{P}_{CG} \times m\mathbf{g}\}^T$ is the gravity wrench vector, where $^P\mathbf{P}_{CG}$ is the moment arm vector from the platform control point P to the platform CG, expressed in frame $\{P\}$ coordinates. This set of pseudostatics equations is expressly for Design Candidate 3, shown in Figure No.2b (and Figure No.3); it is easily modified for the other 5 design candidates.

Considering six-d of are controlled for the platform (3 translations and 3 rotations) using eight independent cables, there are two actuation-redundant cables, which can be used for cable tension optimization (minimizing the least squares measure of all 8 cable tension, while enforcing the constraint of non-negative tensions). MATLAB function lsqnonneg is used for this purpose.

Stiffness calculations
Stiffness analysis for cable-suspended robots was developed by[12], not shown due to space limitations. These calculations require the pseudostatics Jacobian matrix for configuration-dependent translational and rotational stiffness calculations, plus assumptions of cable diameters and Young's Modulus. By using equal parameters amongst the six design candidates, conclusions may be drawn regarding the designs with the highest translational and rotational stiffness, a desired characteristic for ARGOS.

Cable Interference Detection
In general all 6 eight-cable robot designs presented in this paper have the possibility of unwanted cable interference during regular motions, especially for the crossed-cable cases. This section presents an analytical method to detect cable interference between any two of the eight active cables. This method is adapted from[13].

The basic idea is that the common normal between two spatial cables gives the shortest distance between them. The common normal direction is simply found from the cross product between the two cable length vectors. The common normal distance will be found using a vector loop-closure equation. If this distance goes to zero, that is the moment of interference (ignoring the cables' diameter). More practically, if the sign of this distance changes during a trajectory, this identifies cable interference has occurred and the normal IPK solution will not be valid after the sign switch. Figure No.4 shows two spatial cables that can interfere with each other.

B_m and B_n are the two involved fixed base overhead cable reel points; P_m and P_n are the two involved moving platform cable connection points; L_i and L_j are the two total cable lengths, between B_m, P_n and B_n, P_m, respectively; l_i is the length along L_i to the common normal and l_j is the length along L_j to the common normal; and l_{ij} is the length along the common normal between cables i and j. Absolute vectors to points B_m, B_n, P_m, and P_n, plus the cable lengths L_i and L_j are already known from kinematics analysis and the IPK solution. The applicable vector loop-closure equation is (we choose to use $\{0\}$ as the basis for all vectors):

$$\mathbf{l}_i + \mathbf{l}_{ij} - \mathbf{l}_j = \mathbf{P}_m - \mathbf{P}_n \tag{3}$$

Where:

$$\mathbf{l}_i = l_i\hat{\mathbf{l}}_i \qquad \mathbf{l}_j = l_j\hat{\mathbf{l}}_j$$

$$\mathbf{l}_{ij} = l_{ij}\hat{\mathbf{l}}_{ij} \tag{4}$$

$$\hat{\mathbf{l}}_i = \frac{\mathbf{B}_m - \mathbf{P}_n}{\|\mathbf{B}_m - \mathbf{P}_n\|} \qquad \hat{\mathbf{l}}_j = \frac{\mathbf{B}_n - \mathbf{P}_m}{\|\mathbf{B}_n - \mathbf{P}_m\|}$$

$$\hat{\mathbf{l}}_{ij} = \frac{\mathbf{L}_i \times \mathbf{L}_j}{\|\mathbf{L}_i \times \mathbf{L}_j\|}$$

The vector loop-closure equation yields three linear equations to solve for the three unknowns l_i, l_j, and l_{ij}

$$\begin{bmatrix} \hat{l}_{ix} & -\hat{l}_{jx} & \hat{l}_{ijx} \\ \hat{l}_{iy} & -\hat{l}_{jy} & \hat{l}_{ijy} \\ \hat{l}_{iz} & -\hat{l}_{jz} & \hat{l}_{ijz} \end{bmatrix} \begin{Bmatrix} l_i \\ l_j \\ l_{ij} \end{Bmatrix} = \begin{Bmatrix} P_{mx} - P_{nx} \\ P_{my} - P_{ny} \\ P_{mz} - P_{nz} \end{Bmatrix} \quad (5)$$

And the solution is

$$\begin{Bmatrix} l_i \\ l_j \\ l_{ij} \end{Bmatrix} = \begin{bmatrix} \hat{l}_{ix} & -\hat{l}_{jx} & \hat{l}_{ijx} \\ \hat{l}_{iy} & -\hat{l}_{jy} & \hat{l}_{ijy} \\ \hat{l}_{iz} & -\hat{l}_{jz} & \hat{l}_{ijz} \end{bmatrix}^{-1} \begin{Bmatrix} P_{mx} - P_{nx} \\ P_{my} - P_{ny} \\ P_{mz} - P_{nz} \end{Bmatrix} \quad (6)$$

Assuming none of the cable pairs are collinear (nor parallel), the above 3 x 3 matrix is guaranteed to be non-singular and thus invertible. Again, if the common-normal distance l_{ij} goes to zero, that defines the onset of interference. When the sign of this shortest distance l_{ij} changes during a trajectory, this means cable interference has occurred between those two cables.

A special case has $l_{ij} = 0$ for all motion; this occurs for non-crossed cables meeting at the same moving platform vertex. In this case there is no cable interference and we also have $l_i = l_j = 0$ in this situation.

In general amongst 8 active cables, there are a total of 28 cable pairs to check for cable interference at each snapshot in a trajectory. In practice, many of these 28 cable pairs will never intersect by design; therefore, it is possible to check a small subset of these for each robot design.

RESULTS AND DISCUSSION
The methods of this paper were implemented in MATLAB simulation, using dimensions of the current ARGOS laboratory at NASA Johnson Space Center. Comparing the translational workspaces, with horizontal platforms ($\alpha = \beta = \gamma = 0$) showed all 6 candidate robot designs were able to maintain positive cable tensions for all eight cables throughout the entire ARGOS workspace. The MATLAB function lsqnonneg was used for positive-only cable tensions optimization. A representative workspace (for Design 1) is shown in Figure No.5 where each green marker represents an end effector position in the robot workspace where all 8 cable tensions are positive. All six designs yielded an equivalent good result regarding positive cable tensions, so this is not a measure to choose a best design. For all six design candidates, this translational workspace shown in Figure No.5 also presents the singularity-free workspace; as long as the planes bounding the cable-suspended robot borders are not approached nor exceeded, no singularities exist.

The ARGOS Laboratory is a 3D rectangular space with the base frame composed of length $L = 12.50$, width $W = 7.32$, and height $H = 7.62$ m. The rectangular moving platform dimensions of length $l = 1.56$ and width $w = 0.91$ m were chosen to be 1/8 of the ARGOS base frame footprint. These terms are easily changeable according to specific design needs. The moving platform thickness h can be much smaller and is design-dependent. The assumed platform mass m is 100 kg.

The base frame {0} and the moving platform frame {P} were shown in Figure No.2b. The base frame is fixed to the center of the ARGOS footprint, on the floor. The moving frame is fixed to the center of the top of the moving platform.

Now two general trajectories are presented to exercise the robot in MATLAB simulation, for all six designs.

Trajectory 1
Straight-line translation on a diagonal covering most of the reachable workspace, plus rotations about three axes. The initial and final poses $\{x \quad y \quad z \quad \alpha \quad \beta \quad \gamma\}$ for this first trajectory are:

$\{-4.834 \quad 1.596 \quad 0.500 \quad 0 \quad 0 \quad 0\}$

$\{4.834 \quad -1.596 \quad 6.000 \quad 20 \quad 20 \quad 20\}$

Where the position vector $\{^0P_P\} = \{x \quad y \quad z\}^T$ gives the position of control point P with respect to the {0} origin, expressed in {0} coordinates, and the *Z-Y-X* Euler Angles are α, β, γ.

These initial and final moving platform poses are divided into equal Cartesian steps to ensure smooth motion from start to finish, using IPK, pseudostatics, stiffness, and cable-interference-detection calculations at each step. The final pose for Trajectory 1 is shown in Figure No.6, for Design 3.
Trajectory 2

The translational trajectory follows an *XY* circle, with an oscillatory sine wave for *Z* motion. At the same time, the Euler Angles are also varying in an oscillatory manner. The motion data for this second trajectory are:

Circle center	$\{0 \quad 0 \quad 4\}^T$ m
Circle radius	2 m
Z amplitude	±1 m
Z frequency	3 cycles
$\{\alpha \quad \beta \quad \gamma\}$ Amplitude	$\{\pm 15° \quad \pm 10° \quad \pm 5°\}$
$\{\alpha \quad \beta \quad \gamma\}$ Frequency	$\{1 \quad 2 \quad 3\}$ cycles

Again, the circular moving platform poses are divided into equal Cartesian steps to ensure smooth motion from start to finish, using IPK, pseudostatics, stiffness, and cable-interference-detection calculations at each step. Trajectory 2 is shown in Figure No.7, for Design 3.

The cable tension norms for each robot design during the two simulated trajectories are shown in Figures No.8 and 9. Figure 8 shows the square platform with uncrossed cables (Design 5), and the rotated rectangular platform with crossed cables (Design 4) were the best suited to the linear trajectory while the rotated rectangular platform with either uncrossed or crossed cables (Designs 3 and 4, respectively), and the square platform with uncrossed cables (Design 5) were best suited to the circular trajectory. These design candidates were best suited to their respective trajectories due to their relatively low magnitude of cable tensions norms as well as their smooth plot shape corresponding to small overall changes in cable tensions over the course of the simulated trajectory.

It was concluded by visual inspection of the motion animations that the uncrossed cable orientations (Designs 1, 3, and 5) were not subject to cable interference in either of the two simulated trajectories. Figure No.10 and 11 present the distance between cables 2 and 3, plus 6 and 7 for all robot designs that have crossed cables (Designs 2, 4, and 6). It can be seen that all 3 crossed cable designs encounter cable interference while performing the circular trajectory, while avoiding cable interference during the linear trajectory (after the start).

Design 4 had the smallest distance between both cables 2 and 3 and 6 and 7, corresponding to the smallest range of motion before cable interference occurs.

Standard stiffness analysis was performed for all 6 design candidates a 'laUnger *et al.* (1988), not shown. Generally, all 6 designs performed similarly with regards to translational stiffness, hence not giving a means to choose the best design. However, the rotational stiffness is far superior for the cross-cable Designs 2, 4, and 6, compared to that of the uncrossed cable Designs 1, 3, and 6. This is a tradeoff in design; the better rotational stiffness is offset by the unacceptable performance with regards to cable interference.

The results from the cable tension norms and cable interference plots for the generated trajectories show that while some of the crossed cable configurations are better for cable tension optimization and rotational stiffness, their susceptibility to cable interference ultimately eliminate them as a viable option for an improved ARGOS system. The orientation that performed best considering the tested parameters was the square platform with uncrossed cables (Design 5).
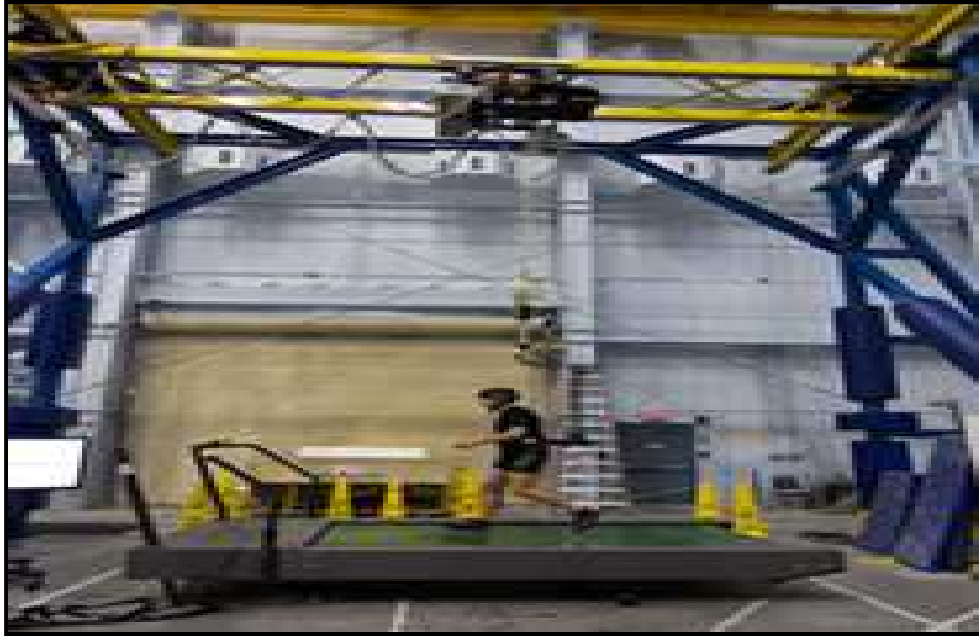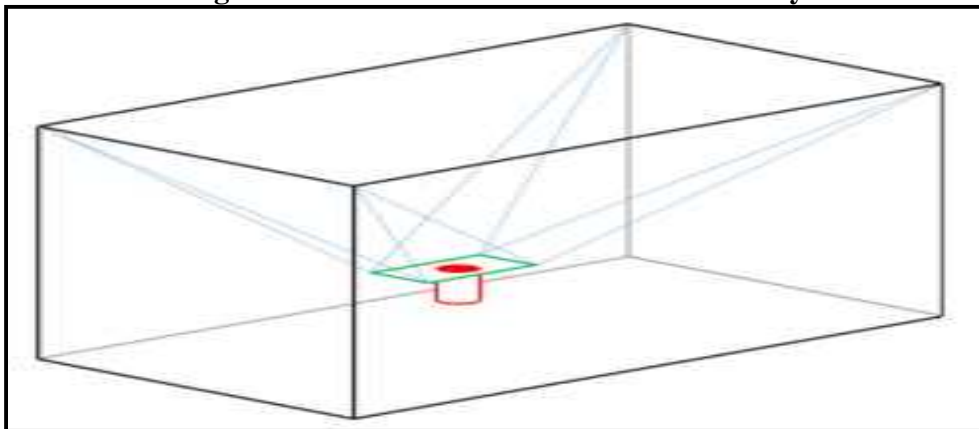
Figure No.1: NASA JSC ARGOS Laboratory

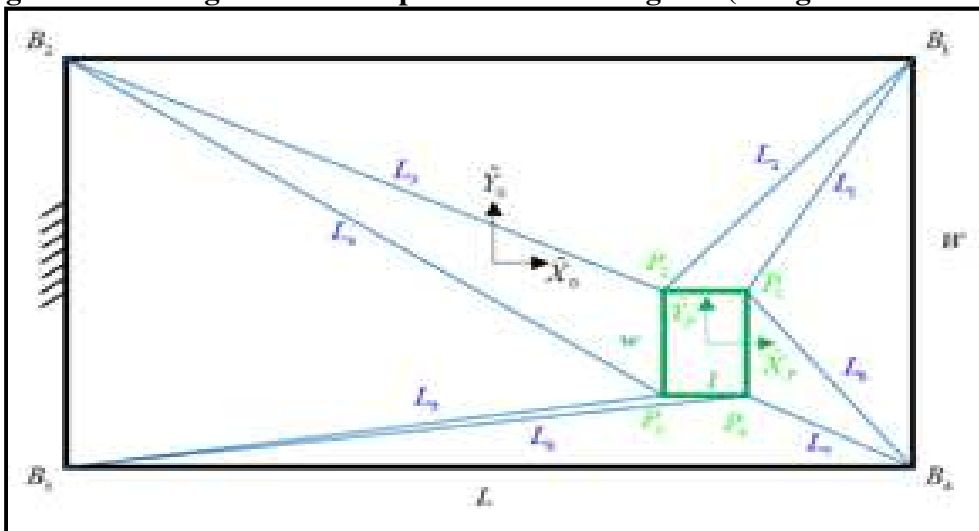**Figure No.2a: Eight-Cable-Suspended Robot Diagram (Design Candidate 1)**

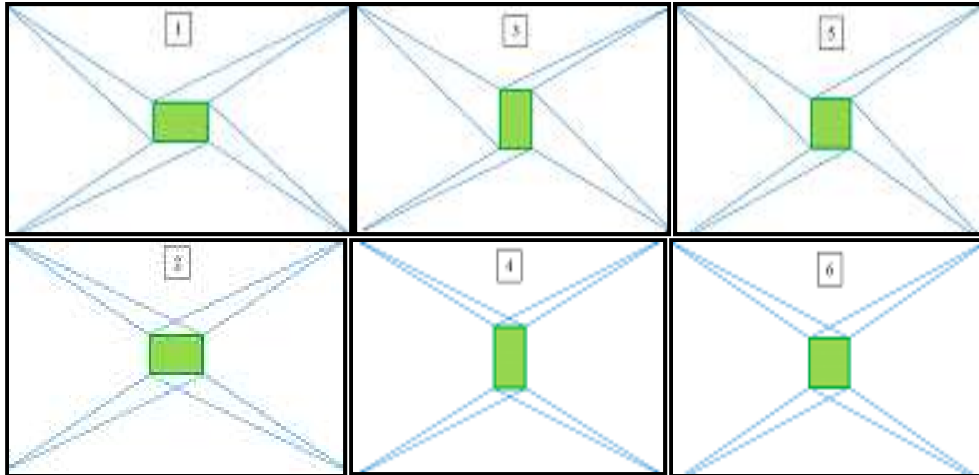**Figure No.2b: Top-View Kinematic Diagram(Design Candidate 3)**

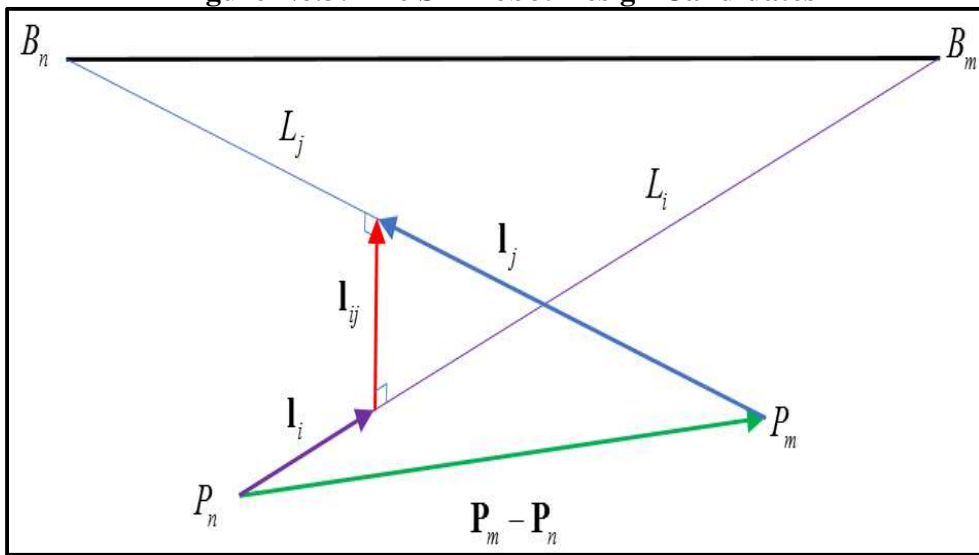**Figure No.3: The Six Robot Design Candidates**

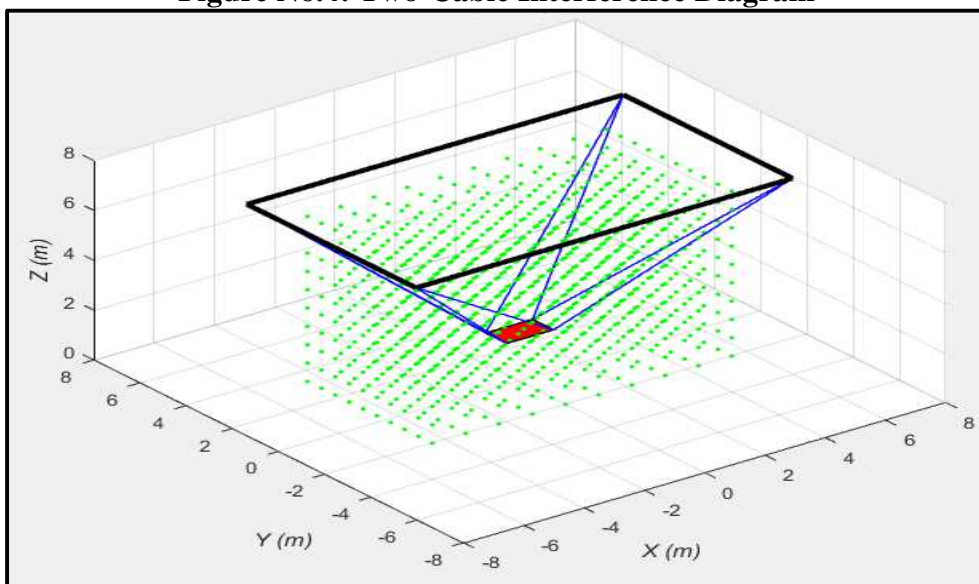**Figure No.4: Two-Cable Interference Diagram**
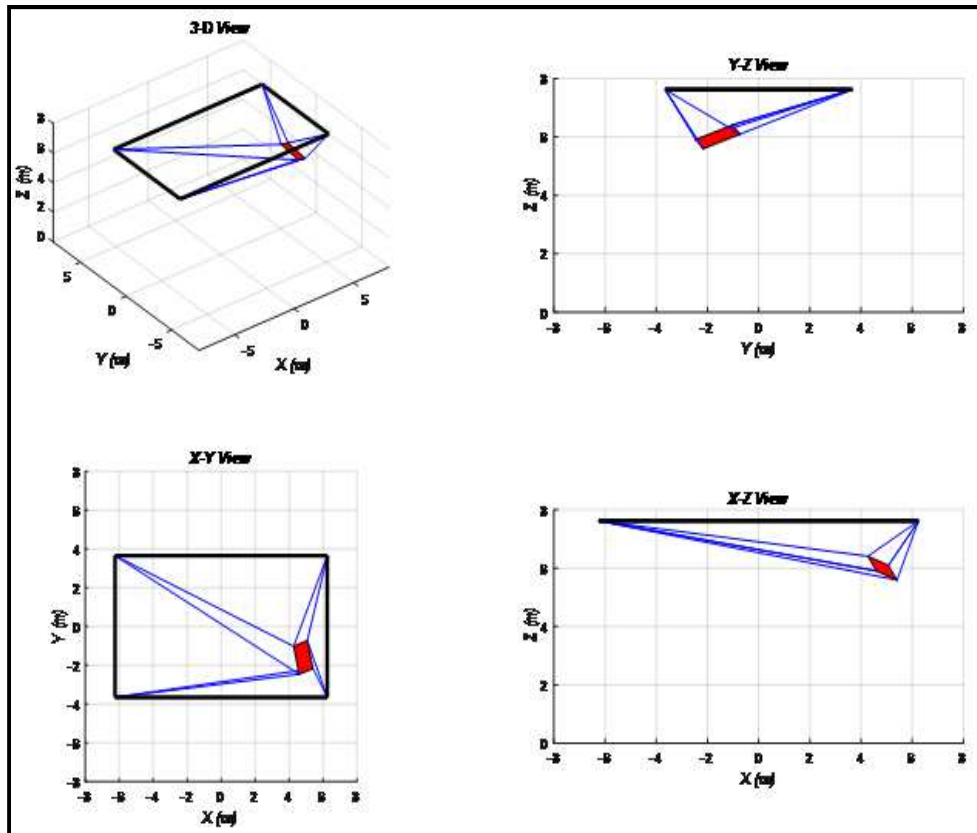

Figure No.5: All-Positive-Cable-Tension Workspace
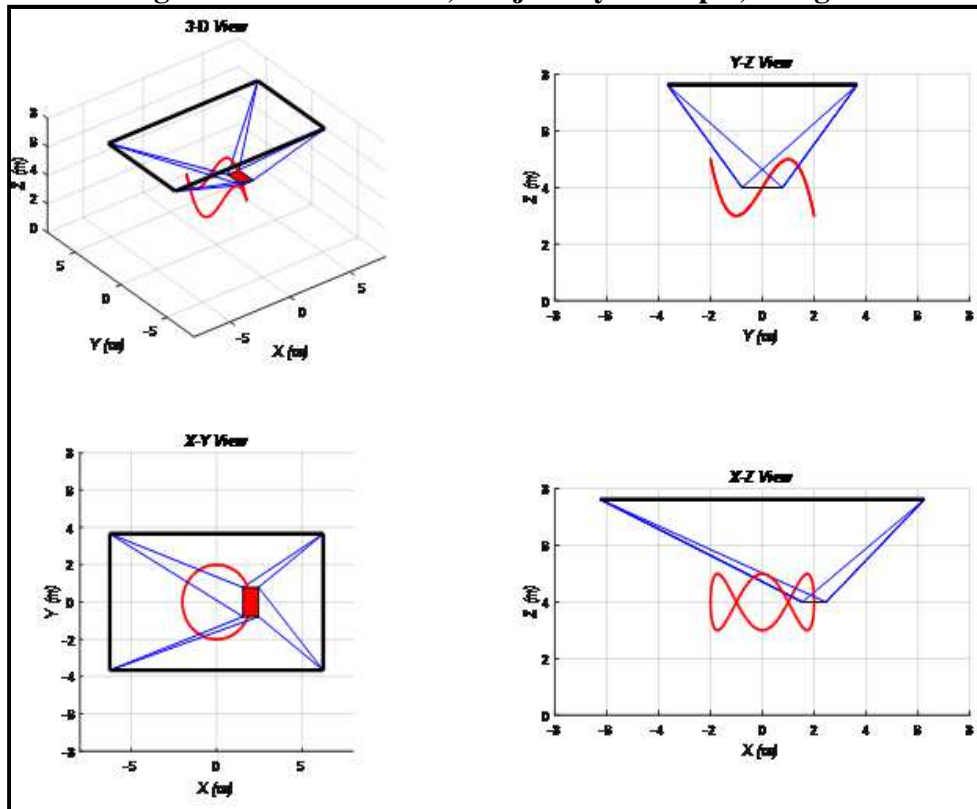
Figure No.6: Final Pose, Trajectory Example, Design 3
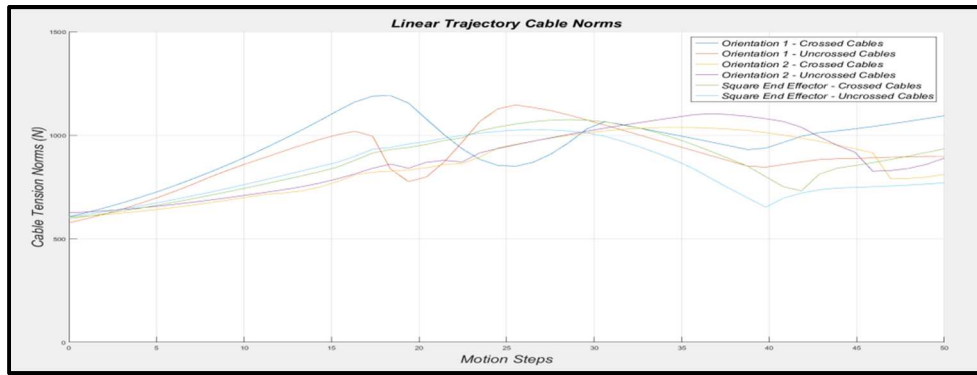

Figure No.7: Circular Trajectory Example, Design 3

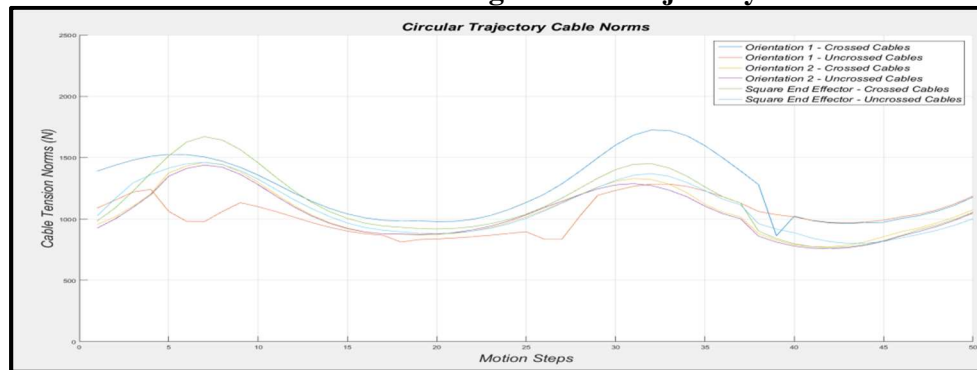**Figure No.8: Cable Tension Norms during Linear Trajectory for each Robot Design**

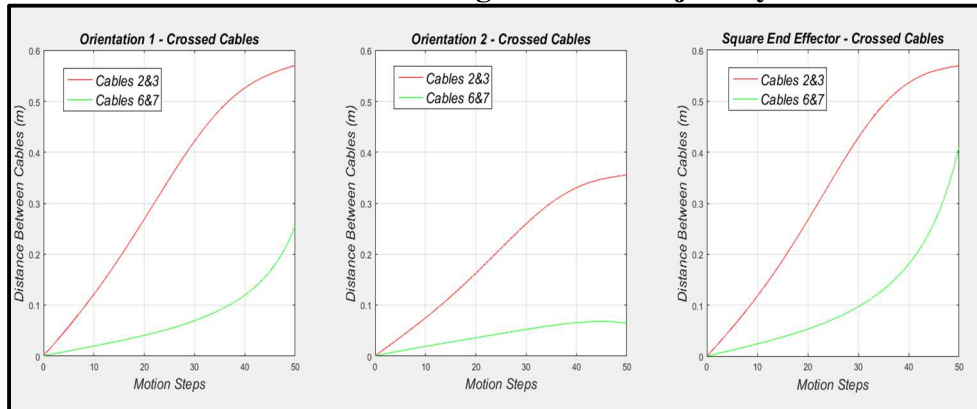**Figure No.9: Cable Tension Norms during Circular Trajectory for each Robot Design**

Figure No.10: Distances between Cables 2-3 and 6-7, Linear Trajectory no cable interference after start
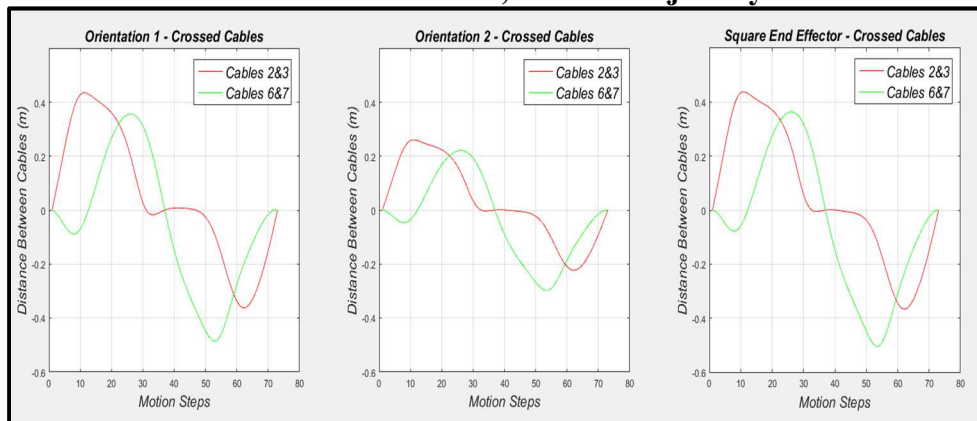

Figure No.11: Distances between Cables 2-3 and 6-7, Circular Trajectory cable interference occurs

CONCLUSION AND RECOMMENDATION

This paper has presented an extension of the triangular 6-cable NIST RoboCrane to a rectangular 8-cable-suspended robot, for use in the ARGOS (Active Response Gravity Offload System) Laboratory at NASA Johnson Space Center. Six candidate cable/platform design arrangements were considered and evaluated in MATLAB simulation, based on all-eight-cable-positive tensions workspace, singularities, magnitude and slope of cable tensions during trajectories, translational/rotational stiffness, and cable interference. Ideal, massless, tensioned, straight-line cable models were used throughout, rather than the quite complicated cable sag models available. Tradeoffs were noted in the design evaluation measures amongst the six candidate 8-cable-suspended robot designs. The overall recommendation based on this work is Design 5 (square platform with uncrossed cables). This is based on only two trajectories, however, the authors expect this to be a general design recommendation result for more general ARGOS trajectories.

The main benefit of our 8-cable RoboCrane extension is that is naturally fits a rectangular room better than the original. The cost is extra motors, cables, and sensors. Additional benefits may be discovered with future work.

Future work plans include

1. Extending our designs to include 4 down-pulling cables; this may have stiffness benefits and will allow downward accelerations in excess of 1-Earth-G (not necessary for standard ARGOS reduced-gravity experiments), but cable interference may be worse.

2. Based on NASA feedback, focus solely on pure translational motion trajectories as Cartesian rotations with the cable-suspended robot are of less importance to ARGOS.

3. Modeling and simulating dynamics for cases where pseudostatics analysis is not sufficient.

4. Implementing project results in scale-hardware prototypes at Ohio University and NASA JSC.

5. Supporting development and implementation of the full-size hardware in ARGOS at NASA JSC, including safe and effective positive-cable-tension-only controller and cable interference avoidance.

CONFLICT OF INTEREST

We declare that we have no conflict of interest.

BIBLIOGRAPHY

1. J. Albus, Bostelman R, and Dagalakis N. "The NIST RoboCrane", *Journal of National Institute of Standards and Technology,* 10(5), 1993, 709-724.
2. Kawamura S, Choe W, Tanaka S and Pandian S. "Development of an ultrahigh speed robot FALCON using wire drive system," *Proceedings of the 1993 IEEE International Conference on Robotics and Automation, (Nagoya, Japan),* 1, 1993, 215-220.
3. Gorman J J, Jablokow K W and Cannon D J. "The cable array robot: Theory and experiment", *Proceedings of the 2001 IEEE International Conference on Robotics and Automation,* 3, 2001, 2804-2810.
4. Bonivento C, Eusebi A, Melchiorri C, Montanari M, Vassura G. "WireMan: A portable wire manipulator for touch-rendering of bas-relief virtual surfaces", *Proceedings of the 1997 International Conference on Advanced Robotics (ICAR 97),* 1997, 13-18.
5. Williams II R L. "Cable-Suspended Haptic Interface", *International Journal of Virtual Reality,* 3(3), 1998, 13-21.
6. Campbell P D, Swaim P L and Thompson C J. "Charlotte Robot Technology for Space and Terrestrial Applications", *25th International Conference on Environmental Systems, San Diego,* 1995.
7. Havlík S. "A cable suspended robotic manipulatorfor large workspace operations", *Journal of Computer-Aided Civil and*

Infrastructure Engineering, 15(6), 2000, 56-68.

8. Bosscher P M, Williams II R L, Bryson L S and Castro-Lacouture D. "Cable-Suspended Robotic Contour Crafting System", *Journal of Automation in Construction,* 17, 2007, 45-55.

9. Williams II R L, Albus J S and Bostelman R V. "Self-Contained Automated Construction Deposition System", *Automation in Construction,* 13(3), 2004, 393-407.

10. Sridhar D and Williams II R L. "Kinematics and Statics including Cable Sag for Large Cable-Suspended Robots", *Proceedings of the ASME IDETC/CIE, Charlotte NC,* August 2016, 21-24, DETC2016-60495.

11. Craig J J. Introduction to Robotics: Mechanics and Control, *Addison Wesley Publishing Co., Reading, MA,* 3rd Edition, 2005, 167.

12. Unger D, Dagalakis N G, Tsai T M and Lee J D. "Optimum stiffness study for a parallel link robot crane under horizontal force", *Symp. on Robotics and Manufacturing, Albuquerque NM,* 2nd Int, 1988, 1037-1046.

13. Otis M, Perreault S, Nguyen-Dang T, Lambert P, Gouttefarde M, Laurendeau D and Gosselin C. Determination and Management of Cable Interferences Between Two 6-DOF Foot Platforms in a Cable-Driven Locomotion Interface, IEEE Transactions on Systems, Man, and Cybernetics – Part A, *Systems and Humans,* 39(3), 2009, 528-544.